Journal of Engineering and Applied Sciences 2 (11): 1627-1639, 2007
ISSN: 1816-949X

Determination of Areal Anisotropy from a Single Vertical Pressure Test and Geological Data in Elongated Reservoirs

[1]Freddy Humberto Escobar, [2]Djebbar Tiab and [1]Lida Vanessa Tovar
[1]Universidad Surcolombiana, Av. Pastrana-Cra. 1, Neiva (Huila-Colombia)
[2]The University of Oklahoma, 100 E. Boyd St. SEC Rm T202, Norman, OK, 73019 USA

Abstract: Elongated reservoirs, resulting mainly from fluvial deposition or faulting, are often found in the three Basins of the Magdalena River Valley in Colombia and several other places around the globe. Since most of these reservoirs are due to parallel stratigraphic or structural features, horizontal permeability anisotropy may occur. Normally, a single horizontal well test is meant to be enough for permeability anisotropy determination. It is not the same situation for vertical wells where interference testing involves at least three active wells. However, in channel-type reservoirs when its width is known from estructural maps or seismic data, the advantage of having, first, radial flow regime which involves two directional permeability and then, linear flow regime related to permeability in one direction, the horizontal anisotropy can be also determined from a single well pressure test. In this study, a detailed analysis of pressure derivative behavior for a vertical well in areally anisotropic long and narrow reservoirs is presented for the case of constant rate production. For this case, the radial flow is distorted into an elliptical flow profile and its shape is determined by the maximum and minimum principle permeabilities. The elliptical nature of the system leads to the determination of a bi-dimensional permeability while the linear flow allows for the estimation of permeability in a single direction. The proposed interpretation method uses the concept of the TDS technique, which relies on characteristic points and straight lines corresponding to flow regimes found on the loglog plot of pressure and pressure derivative to caculate various reservoir parameters directlty, thus avoiding the use of type-curve matching or regression analysis. The technique was successfully verified by interpreting synthetic pressure tests for oil reservoirs.

Key words: Areal anisotropy, radial flow, parabolic flow, dual linear flow, single linear flow, maximum and minimum principal permeabilities

INTRODUCTION

In oil and gas reservoirs, it is generally accepted that vertical and horizontal permeabilities are different. Commonly, the fact that horizontal permeability varies from one direction to another is ignored. This horizontal anisotropy generally results from the deposition environment, sedimentary processes or tectonism. This last one may cause oriented fractures so that permeability can dominate along one direction. Permeability measured along the bedding plane can be several times higher than the one measured normal to the stratum. This vertical/ horizontal anisotropy is often considered in partially completed wells. It is costumary to neglect horizontal permeability in transient pressure analysis of vertical wells, mainly, because its effect cannot be identified in the pressure or pressure derivative curves. As a result, interference testing involving at least three active wells is recommended. Therefore, determination of the directional permeabilities from a single well test analysis conducted in a vertical well has been a challenge issue to the field of well test interpretation for several decades. Meanwhile, a single pressure test conducted in a horizontal may lead to the estimation of reservoir permeability anisotropy due to the fact of finding a variety of flow regimes. This advantage can be also applied to vertical wells; for instance, the presence of partial completation or partial penetration in a vertical well pressure tests can be used to estimate vertical permeability. Long and narrow reservoirs formed by either faulting or fluvial deposition are not the exception to the rule as long as reservoir width is known and linear flow develops.

Characterization of channel reservoirs using type curves of pressure and pressure derivative began in earnest in the seventies (Tiab, 1975, 1976, 1979). Recently several researchers have revisited these systems, particularly Escobar *et al.* (2005), Nutakki and Mattar (1982) and Wong *et al.* (1986). Escobar *et al.* (2007)

Corresponding Author: Freddy Humberto Escobar, Universidad Surcolombiana, Av. Pastrana-Cra. 1, Neiva (Huila-Colombia)

presented a set of equations and a methodology to characterize elongated isotropic reservoirs from well test analysis by means of the TDS technique, which was developed by Tiab (1993, 1995). By combination of the TDS technique, conventional analysis and non-linear regression, Sui *et al.* (2007) presented a methodology to estimate reservoir anisotropy in elongated reservoirs.

Reservoirs width may be known from either geological or seismic data, even though anisotropy may affect this last measurement. As long as the linear flow regime develops for cases of either long duration test, high reservoir permeability, or small reservoirs, horizontal anisotropy can be obtained from the linear flow regime. This is very attractive for small channels in which drilling other wells, for obvious reasons, is not feasible; then, interference testing may never take place for anisotropy determination. Here, a methodology is presented to estimate horizontal reservoir anisotropy in channel-type reservoirs based upon the TDS technique and using only the pressure and pressure derivative plot. The proposed methodology is verified with synthetic examples. For further information on the TDS, Tiab's Direct Synthesis, technique the reader is invited to refer to Tiab (1993, 1995), Tiab *et al.* (1999) and Escobar *et al.* (2007).

MATHEMATICAL TREATMENT

Basic equations: Let us define dimensional quantities. Starting with dimensional time:

$$t_D = \frac{0.0002637\bar{k}t}{\phi\mu c_t r_w^{\ 2}} \tag{1}$$

$$t_{DA} = \frac{0.0002637\bar{k}t}{\phi\mu c_t A} \tag{2}$$

$$t_{D_L} = \frac{t_D}{W_D^2} = \frac{0.0002637k_x t}{\phi\mu c_t Y_E^{\ 2}} \tag{3}$$

During the radial flow regime, the permeability and anisotropy are defined by:

$$\bar{k} = \sqrt{k_x k_y} \tag{4}$$

$$A = \frac{k_x}{k_y} \tag{5}$$

Dimensionless reservoir width and well position are (Fig. 1):

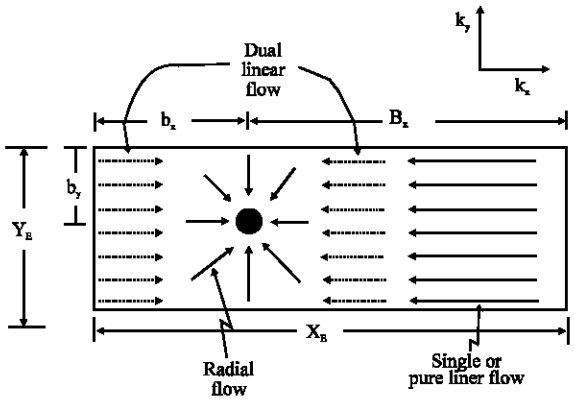

Fig. 1: Reservoir geometry and flow regimes

$$W_D = \frac{Y_E}{r_w} \tag{6a}$$

$$X_D = \frac{2b_x}{X_E} \tag{6b}$$

$$Y_D = \frac{2b_y}{Y_E} \tag{6c}$$

Dimensionless pressure and pressure derivative during radial flow regime or late behavior:

$$P_D = \frac{\bar{k}h}{141.2q\mu B}\Delta P \tag{7}$$

$$t_D * P_D' = \frac{\bar{k}h}{141.2q\mu B}\left(t * \Delta P'\right) \tag{8}$$

During intermediate behavior when linear flow dominates the permeability will be taken in the x direction. Therefore:

$$P_D = \frac{k_x h}{141.2q\mu B}\Delta P \tag{9}$$

$$t_D * P_D' = \frac{k_x h}{141.2q\mu B}\left(t * \Delta P'\right) \tag{10}$$

Governing equations: Many wells have been observed to display long-term linear flow. Linear flow can be detected by a ½-slope line in a log-log plot of the pressure derivative.Linear flow regime is also observed when the well is located at one of the reservoir extremes as depicted in Fig. 1 and 2. This is governed by the following constant rate equation:

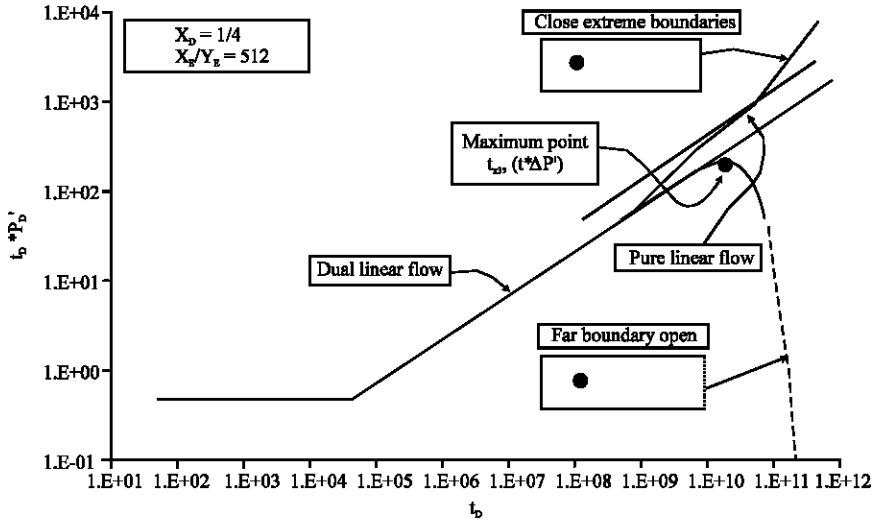

Fig. 2: Pressure derivative behavior for a well (a) both extreme boundaries are close, (b) close near boundary and open far boundary

$$P_D = 2\pi\sqrt{t_{D_L}} + S_L = \frac{2\pi\sqrt{t_D}}{W_D} + S_L \tag{11}$$

As long as the well is located far away from one of the extreme boundaries, dual-linear flow is developed before the linear flow. In this case, the governing equation is:

$$P_D = 2\sqrt{\pi t_{D_L}} + S_{DL} = \frac{2\sqrt{\pi t_D}}{W_D} + S_{DL} \tag{12}$$

The subscripts L and DL in Eq. 11 and 12 stand for linear and dual-linear flow regimes. Pressure derivatives for Eq. 11 and 12 are, respectively:

$$(t_D * P_D')_L = \frac{\pi\sqrt{t_D}}{W_D} \tag{13}$$

$$(t_D * P_D')_{DL} = \frac{\sqrt{\pi t_D}}{W_D} \tag{14}$$

As observed in Fig. 3, parabolic flow, characterized by a slope of -½ of pressure derivative curve, develops as a result of the simultaneous effect of an open boundary near the well and the expected linear flow regime along the far lateral side of the reservoir (Escobar *et al*., 2005). The pressure and pressure derivative governing equations for this flow regime are, respectively (Escobar *et al*., 2007):

$$P_D = -(W_D)(X_D)^2\left(\frac{X_E}{Y_E}\right)^2 t_D^{-0.5} + s_{PB} \tag{15}$$

$$t_D * P'_D = \frac{W_D}{2}(X_D)^2\left(\frac{X_E}{Y_E}\right)^2 t_D^{-0.5} \tag{16}$$

Dual-linear and linear flows take place when the well is off-centered with respect the reservoir's extreme lateral sides. The inflection point during the transition period from dual-linear to linear flows is governed by the following relationship according to Escobar *et al*. (2007):

$$(t_D * P_D')_F = \frac{\pi + \sqrt{\pi}}{2W_D} * t_D^{0.5} \tag{17}$$

$$t_{D_F} = \frac{W_D^2 X_D}{\sqrt{\pi}}\left(\frac{X_E}{Y_E}\right)^2 \tag{18}$$

Characteristic lines and points: Tiab (1993) obtained a practical equation to estimate reservoir permeability from the radial flow regime when the dimensionless pressure derivative is one half:

$$\bar{k} = \frac{70.6q\mu B}{h(t*\Delta P')_r} \tag{19}$$

As shown in Fig. 4, the intersection point between the radial-flow line and the linear-flow line, t_{RLi}, is unique. At this point of intersection, the dimensionless pressure derivative takes a value of one half when the well is centered regarding the reservoir's parallel boundaries. Same situation applies to dual-linear flow. Based upon this observation Eq. 13 and 14 become:

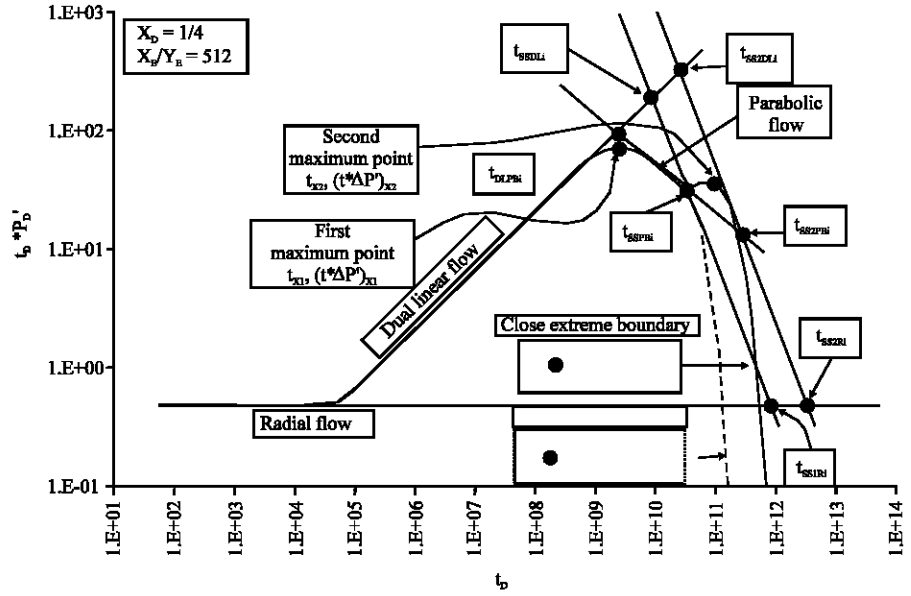

Fig. 3: Characteristic points of the parabolic flow

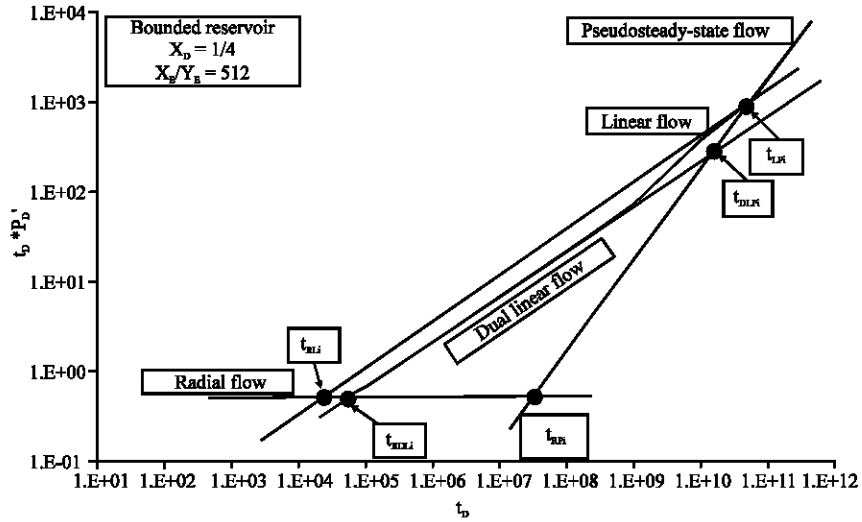

Fig. 4: Pseudosteady-state line intersection with either linear, dual-linear or radial flow lines

$$\frac{\sqrt{\pi t_D}}{W_D}\Big|_{DL} = 0.5 \quad (20)$$

$$\frac{\pi\sqrt{t_D}}{W_D}\Big|_{L} = 0.5 \quad (21)$$

Figure 3 describes the transient pressure behavior for a well in a channel when areal anisotropy is considered. The beginning of linear flow and consequently ending of radial flow, is a function of the permeability in the y direction. Replacing the dimensionless parameters, Eq. 1 and 6c and solving for k_y yields:

$$k_y = \frac{301.77\phi\mu c_t Y_E^2}{t_{RDL_i}} \quad (22)$$

$$k_y = \frac{90.06\phi\mu c_t Y_E^2}{t_{RL_i}} \quad (23)$$

Both linear flow and dual linear flow are developed along the x direction. Therefore, substitution of Eq. 1, 6 and 8 into Eq. 22 and 23 provides solutions for k_x:

$$k_x = \left(\frac{7.2034qB}{Y_E h(t*\Delta P')_L}\right)^2 \frac{\Delta t_L \mu}{\phi c_t} \quad (24)$$

$$k_x = \left(\frac{4.064qB}{Y_E h\left(t*\Delta P'\right)_{DL}}\right)^2 \frac{\Delta t_{DL}\mu}{\phi c_t} \quad (25)$$

When the pressure derivative value is read at the time, $\Delta t = 1$ hr, extrapolated if necessary, Eq. 24 and 25 will then become:

$$k_x = \left(\frac{7.2034qB}{Y_E h\left(t*\Delta P'\right)_{L1}}\right)^2 \frac{\mu}{\phi c_t} \quad (26)$$

$$k_x = \left(\frac{4.064qB}{Y_E h\left(t*\Delta P'\right)_{DL1}}\right)^2 \frac{\mu}{\phi c_t} \quad (27)$$

As for the case of parabolic flow, replacing the dimensionless parameters in Eq. 16 will result in a relationship to obtain either permeability, reservoir width or well location, as preferred:

$$\frac{k_x^{1.5} Y_E}{b_x^2} = 17390\left[\frac{q\mu B}{h\left(t*\Delta P'\right)_{PB}}\right]\left[\frac{\phi\mu c_t}{t_{PB}}\right]^{0.5} \quad (28)$$

Where, $(t*\Delta P)_{PB}$ is the pressure derivative during parabolic flow read at any convenient time, t_{PB}.

Intersection of dual-linear, linear and radial lines with pseudosteady-state line: For long producing times in a closed reservoir the pressure derivative is characterized by a unit-slope line which is given by:

$$\left(t_D * P_D'\right)_P = 2\pi * t_{DA} \quad (29)$$

As expressed by Tiab (1993) the time of intersection of the pseudosteady-state line with the radial flow line (t_{RPi}) can be used to calculate the drainage area:

$$A = \frac{\overline{k}t_{RPi}}{301.77\phi\mu c_t} \quad (30)$$

Also, the times of intersection of the pseudosteady-state line with the linear and dual-linear pressure derivative lines (Fig. 4) can also be used to estimate the reservoir area.

$$A = \sqrt{\frac{k_x t_{DLP_i} Y_E^2}{301.77\phi\mu c_t}} \quad (31)$$

$$A = \sqrt{\frac{k_x t_{LP_i} Y_E^2}{948.047\phi\mu c_t}} \quad (32)$$

Equation 31 and 32 are obtained by combining Eq. 13, 14 and 29 and substituting for the dimensionless terms.

Intersection between the parabolic-flow line with either dual-linear or radial-flow lines: Parabolic flow only takes place when the well is near the constant pressure boundary. Equating Eq. 16 with 13 will result in Eq. 33 after replacing the dimensionless quantities and solving explicitely for b_x:

$$b_x = \frac{1}{65.41}\sqrt{\frac{k_x t_{DLPB_i}}{\phi\mu c_t}} \quad (33)$$

Equating Eq. 16 to 0.5 and plugging the dimensionless parameters yields:

$$b_x = \sqrt{\left(\frac{Y_E}{246.32}\right)\sqrt{\frac{k_x t_{RPB_i}}{\phi\mu c_t}}} \quad (34)$$

Intersection between the constant-pressure line with either dual-linear, radial or parabolic lines: When the two extreme sides of a rectangular reservoir are constant-pressure boundaries Escobar *et al.* (2007) showed (Fig. 3) that a straight line of slope = -1 represents the parabolic flow regime. The governing equation for this line is:

$$t_D * P_D' = \left(\frac{W_D^2}{\pi^2}\right)\left(X_D^{1.5}\right)\left(\frac{X_E}{Y_E}\right)^3 \left(t_D^{-1}\right) \quad (35)$$

For the mixed boundary case, the governing equation is:

$$t_D * P_D' = \left(\frac{W_D^2}{\pi}\right)\left(X_D^{1.5}\right)\left(\frac{X_E}{Y_E}\right)^3 \left(t_D^{-1}\right) \quad (36)$$

Equating Eq. 35 and 36 with Eq. 14 and the dimensionless value of the pressure derivative during the infinite-acting period, $(t_D*P_D') = 0.5$, the following relationships are obtained once the respective dimensionless quantities are replaced:

Intersection of the first constant pressure line (slope=-1) and the dual-linear flow line:

$$X_E^3 = \left(\frac{1}{1.426\times10^9}\right)\left(\frac{k_x t_{SS_1DL_i}}{\phi\mu c_t}\right)^3\left(\frac{1}{b_x^3}\right) \quad (37)$$

Intersection of the first constant pressure line (slope=-1) line and the radial flow line:

$$X_E^3 = \left(\frac{1}{4.72\times10^6}\right)\left(\frac{k_x t_{SS_1R_i}}{\phi\mu c_t}\right)^2\left(\frac{Y_E^2}{b_x^3}\right) \quad (38)$$

Intersection of the first constant pressure line (slope=-1) and parabolic lines:

$$X_E^3 = \frac{1}{77.9}\left(\frac{k_x t_{SS_1PB_i}}{\phi\mu c_t}\right)b_x \quad (39)$$

The subscript SS_1 stands for the first straight line (of slope=-1) observed.

Intersection of the second constant pressure line (slope=-1) and dual-linear lines:

$$X_E^3 = \left(\frac{1}{1.42\times10^{10}}\right)\left(\frac{k_x t_{SS_2DL_i}}{\phi\mu c_t}\right)^3\left(\frac{1}{b_x^3}\right) \quad (40)$$

Intersection of the second constant pressure line (slope=-1) and radial lines:

$$X_E^3 = \left(\frac{1}{4.66\times10^7}\right)\left(\frac{k_x t_{SS_2R_i}}{\phi\mu c_t}\right)^2\left(\frac{Y_E^2}{b_x^3}\right) \quad (41)$$

Intersection of the second constant pressure line (slope=-1) and parabolic lines:

$$X_E^3 = \frac{1}{768.4}\left(\frac{k_x t_{SS_2PB_i}}{\phi\mu c_t}\right)b_x \quad (42)$$

Suffix SS2 stands for the second -1-slope line observed.

The inflection point between the transition of the linear flow periods is useful for estimation of the well position, b_x. Combining Eq. 17, 18, 1 and 10 and solving for the well position, yields:

$$b_x = \frac{1}{135813.52X_E}\left(\frac{Y_E k_x h(t*\Delta P')_F}{q\mu B}\right)^2 \quad (43)$$

$$b_x = \sqrt{\frac{k_x t_F}{5448.2\phi\mu c_t}} \quad (44)$$

Maximum points

Well near the constant pressure boundary: As seen in Fig. 3, at later times, the pressure derivative curve displays two maximum points when the reservoir has mixed boundaries and the well is near the open one. The first maximum takes place when dual-linear flow ends and the parabolic flow follows. The second maximum point is formed once the parabolic line ends and the no-flow boundary has been reached by the transient wave. The constant-pressure effect still dominates the test. When both extreme sides of the reservoirs are open to flow the pressure derivative behaves in a similar way as for the mixed boundary case. However, no second maximum point is observed. Equations of the maximum points are used to estimate reservoir area and well location.

The first maximum point takes places when a change from dual-linear to parabolic flow regime is attained. The governing equation for this maximum point is given by:

$$(t_D * P_D')_{X1} = \frac{2}{3}\frac{\sqrt{\pi}}{W_D}t_{D_{X1}}^{0.5} \quad (45)$$

$$\frac{X_E}{Y_E} = \frac{2}{3}\left(\frac{\sqrt{\pi}}{W_D X_D}\right)t_{D_{X1}}^{0.5} \quad (46)$$

$$\frac{X_E}{Y_E} = \left(\frac{\sqrt{\pi}}{X_D}\right)(t_D * P_D')_{X1} \quad (47)$$

Figure 3 also displays the second maximum point which occurs at the end of the parabolic-flow line and the start of steady-state line. The equation corresponding to this maximum is:

$$(t_D * P_D')_{X2} = \frac{\sqrt{\pi}}{W_D}\left(X_D^2\right)t_{D_{X2}}^{0,5} \quad (48)$$

$$\frac{X_E}{Y_E} = \left(\frac{\pi}{2W_D}\right)t_{D_{X2}}^{0.5} \quad (49)$$

$$\frac{X_E}{Y_E} = \left(\frac{\sqrt{\pi}}{2X_D^2}\right)(t_D * P_D')_{X2} \quad (50)$$

Substituting the dimensionless quantities into Eq. 45 through 50 and solving for either well position, b_x, or reservoir length, X_E, respectively, yields:

$$b_x = \left(\frac{1}{58.8}\right)\sqrt{\left(\frac{k_x t_{X1}}{\phi\mu c_t}\right)} \quad (51)$$

$$b_x = \frac{k_x h Y_E (t*\Delta P')_{X1}}{159.327q\mu B} \quad (52)$$

$$X_E = 637.3\left(\frac{b_x^2}{Y_E}\right)\left(\frac{q\mu B}{k_x h}\right)\left(\frac{1}{(t*\Delta P')_{X2}}\right) \quad (53)$$

$$X_E = \frac{1}{39.2}\sqrt{\frac{k_x t_{X2}}{\phi\mu c_t}} \quad (54)$$

Well near the no-flow boundary: When an elongated reservoir has mixed boundaries and the well is near the no-flow boundary, the pressure derivative displays a maximum point once the constant pressure boundary is felt as shown in Fig. 1. The governing equation for this maximum point is (Escobar *et al.*, 2007):

$$\frac{X_E}{Y_E} = \frac{\pi^{1.5}}{4}\left(\frac{1}{W_D}\right)t_{D_{X3}}^{0.5} \quad (55)$$

Substituting Eq. 1 and 6 into 55 and solving for the reservoir length, X_E, gives:

$$X_E = \frac{1}{44.24}\left(\frac{k_x t_{X3}}{\phi\mu c_t}\right)^{0.5} \quad (56)$$

Skin factors: The equation to estimate the mechanical skin factor from the radial flow regime was presented by Tiab (1995):

$$s_m = 0.5\left[\frac{(\Delta P)_r}{(t*\Delta P')_r} - \ln\left(\frac{\bar{k}t_r}{\phi\mu c_t r_w^2}\right) + 7.43\right] \quad (57)$$

The skin factor caused by the convergence from radial flow into linear flow is determined by dividing the dimensionless pressure equation by the dimensionless pressure derivative equation. The same procedure is performed for the skin factor due to the convergence from either lineal to dual-linear or lineal to radial flow and from parabolic to dual linear flow. After replacing the dimensionless quantities in these results and solving for the skin factor we obtain:

$$s_L = \left(\frac{\Delta P_L}{(t*\Delta P')_L} - 2\right)\frac{1}{34.743 Y_E}\sqrt{\frac{k_x t_L}{\phi\mu c_t}} \quad (58)$$

$$s_{DL} = \left(\frac{\Delta P_{DL}}{(t*\Delta P')_{DL}} - 2\right)\frac{1}{19.601 Y_E}\sqrt{\frac{k_x t_{DL}}{\phi\mu c_t}} \quad (59)$$

$$s_{PB} = \left(\frac{\Delta P_{PB}}{(t*\Delta P')_{PB}} + 2\right)\left(\frac{123.16 b_x^2}{Y_E}\right)\sqrt{\frac{\phi\mu c_t}{k_x t_{PB}}} \quad (60)$$

Where, ΔP_L, $(t*\Delta P)_L$, ΔP_{DL}, $(t*\Delta P)_{DL}$, ΔP_{PB}, and $(t*\Delta P)_{PB}$ are the pressure and pressure derivative values read on the linear, dual linear and parabolic flow regimes during any convenient time, t_L, t_{DL} and t_{PB}, respectively. The total skin factor is the summation of the linear, dual-linear and mechanical skin factors.

$$s_t = s_m + s_L + s_{DL} \quad (61)$$

$$s_t = s_m + s_{DL} + s_{PB} \quad (62)$$

Reservoir anisotropy: So far, we have assumed that

$$\bar{k} = \sqrt{k_x k_y}$$

therefore, x and y must be the directions of horizontal principal permeability and $k_{Hmax} = \max(k_x, k_y)$, $k_{Hmin} = \min(k_x, k_y)$. However, if

$$\bar{k} \neq \sqrt{k_x k_y}$$

we have to find θ, k_{Hmax} and k_{Hmin}. Ayestaran *et al.* (1989) attempted to combine seismic data and transient pressure data to quantify the large-scale anisotropic permeabilities (Fig. 5). For elongated reservoirs, as long as the reservoir width, Y_E, could be determined from seismic data, k_x and k_y can also be determined by:

$$k_x = \bar{k}\left(\frac{b_x}{b_x'}\right)^2 \quad (63a)$$

$$k_y = \bar{k}\left(\frac{b_y}{b_y'}\right)^2 \quad (63b)$$

When the principal permeability directions are not aligned with the boundary directions, Her-Yuan and Lawrance (2000) presented the following expression to find the angle (θ_i) and maximum and minimum permeability as suggested by Sui *et al.* (2007):

$$\frac{1}{\bar{k}_i} = \frac{\cos^2\theta_i}{k_{max}} + \frac{\text{sen}^2\theta_i}{k_{min}} \quad (64)$$

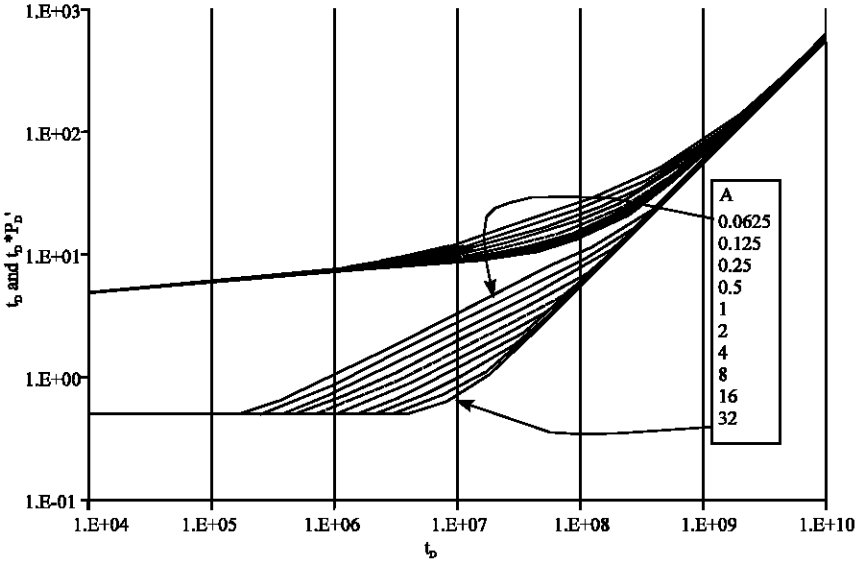

Fig. 5: Pressure and pressure derivative behaviour for a well in a long anisotropic reservoir

Based upon Fig. 6, the following relationship exist between the different angles:

$$\theta_i = \beta_i - \alpha \tag{66}$$

According to Eq. 65, 64 is reformulated as:

$$\frac{1}{\bar{k}_i} = \frac{\cos^2(\beta_i - \alpha)}{k_{max}} + \frac{\text{sen}^2(\beta_i - \alpha)}{k_{min}} \tag{67}$$

Where, $\bar{k}$ is the permeability in some specific direction and θ is the counterclockwise angle with respect to k_{max}. For isotropic reservoir, $k_{max} = k_{min} = \bar{k}$.
If

$$\bar{k} \neq \sqrt{k_x k_y}$$

we can estimate θ, k_{max} and k_{min} by solving the following system based upon Fig. 7:

$$\begin{cases} \dfrac{1}{k_y} = \dfrac{\cos^2(\theta - \beta)}{k_{max}} + \dfrac{\text{sen}^2(\theta - \beta)}{k_{min}} \\ \dfrac{1}{k_x} = \dfrac{\sin^2(\theta \pm \pi/2)}{k_{max}} + \dfrac{\cos^2(\theta \pm \pi/2)}{k_{min}} \\ \bar{k} = \sqrt{k_{H\,max} k_{H\,min}} \\ \dfrac{k_{min}}{k_{max}} = \dfrac{\tan(\theta - \beta)}{\tan\theta} \end{cases} \tag{68}$$

Sui *et al.* (2007) suggested that for cases when the well is off-centered regarding the reservoir's closest

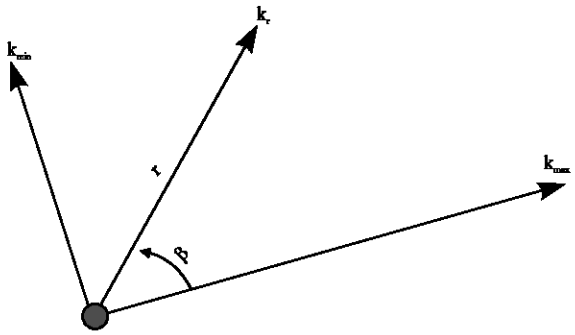

Fig. 6: Permeability configuration, after Her-Yuan and Lawrence (2003)

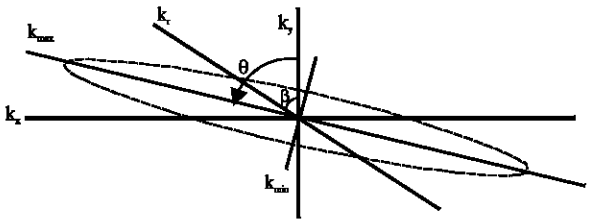

Fig. 7: Well configuration after Sui *et al.* (2007)

parallel boundaries, k_x can be determined with Eq. 24 and/or 25, while k_y is obtained from the following reformulation of Bendekim *et al.* (2002):

$$k_y = \frac{948 b_y^2 \phi \mu c_t}{t_{re} \cos^2\beta} \tag{69}$$

The degree of anisotropy can be estimated from:

$$A = k_{max} / k_{min} \quad (70)$$

STEP-BY-STEP PROCEDURE

The following procedure applies to rectangular reservoirs where the well is located near the closed boundary and the far boundary is either open or closed to flow. The test lasts long enough so that radial, dual-linear, linear and either pseudosteady-state or steady-state flow regimes are well defined.

Step 1: Plot ΔP and t*ΔP' vs. time on a log-log plot.

Step 2: Draw the infinite acting behavior, dual-linear, linear flow and the pseudosteady-state lines. Read the value of $(t*\Delta P')_r$. Choose any convenient time during radial flow regime, t_r and read the corresponding $(\Delta P)_r$ value.

Step 3: Calculate $\bar{k}$ using Eq. 19 and mechanical skin factor, s_m, from Eq. 57.

Step 4: If the well is suspected to be centered regarding the reservoir's closest boundaries, read the intersection of the radial line with the dual linear, t_{DLRi} and linear lines, t_{LRi}, if given the case. Knowing the true reservoir width from seismic data estimate k_y by using Eq. 22 (and 23 if linear flow is present). If the well is off-centered, then read t_{RE} estimate k_y from Eq. 69.

Step 5: Find k_x from Eq. 4 if

$$\bar{k} = \sqrt{k_x k_y}$$

otherwise skip this step.

Step 6: Choose any convenient time on the dual-linear and linear flow lines and read t_{DL}, $(t*\Delta P')_{DL}$, ΔP_{DL} and t_L, $(t*\Delta P')_L$, ΔP_L, respectively. Recalculate k_x with Eq. 24 and 25, respectively, if given the case. If desired an average value of k_x may be estimated. If it is suspected that

$$\bar{k} \neq \sqrt{k_x k_y}$$

solve the system of Eq. 68 and find θ, k_{max} and k_{min}

Step 7: Estimate the geometric skin factors, s_L and s_{DL}, with Eq. 58 and 59.

Step 8: If only dual linear is seen, we assume that the well is centered with respect to the reservoir's lateral boundaries, then, $b_x = 0.5X_E$. Otherwise, for a closed system, read the inflection point t_F, $(t*\Delta P')_F$, between the transition of dual linear and linear flows and estimate well position, bx, from Eq. 43 and 44.

Step 9: Read the intersection time between the pseudosteady-state and radial, dual-linear and linear lines t_{RPi}, t_{DLPi} and t_{RLPi}, respectively. Calculate the reservoir area using Eq. 30 through 32, respectively. Estimate reservoir length, X_E, by A/Y_E.

Step 10: Well is far from the constant pressure boundary. Once the linear flow line vanishes and the effect of the flow boundary becomes dominant, a maximum point on the pressure derivative is observed (Fig. 2). Read the coordinates of this point: t_{X3}, $(t*\Delta P')_{X3}$, and find reservoir length, X_E with Eq. 56.

Step 11: Well is near the constant-pressure boundary. Once the dual linear flow line vanishes and the effect of the flow boundary becomes dominant, the parabolic flow takes place and a maximum point on the pressure derivative is observed (Fig. 3). Read the coordinates of this maximum point: t_{X1}, $(t*\Delta P')_{X1}$, and find well position, b_x with Eq. 51 and 52.

Step 12: Select any convenient time, t_{PB}, on the parabolic flow line and read $(t*\Delta P')_{PB}$ and ΔP_{PB}. Calculate b_x with Eq. 28. Either Y_E or k_x can be verified.

Step 13: Read the intersection time of the parabolic flow with both dual linear and radial flow lines: t_{PBDLi} and t_{PBRi}. Find the distance from the well to the nearest boundary, b_x, using Eq. 33 and 34. Also estimate the parabolic skin factor, s_{PB}, using Eq. 60. Notice that sometimes parabolic flow may not be well developed.

Step 14: Find the total skin factor, s_t, with either Eq. 61 or 62.

Step 15: Well is close to constant-pressure boundary. Refer to Fig. 3. Read the coordinates of the second maximum point: t_{X2} and $(t*\Delta P')_{X2}$ and calculate the reservoir length, X_E, using Eq. 53 and 54. If this maximum point is not clearly observed, it is recommended to estimate X_E using Eq. 40, 41 and/or 42 using the intersection of the -1-slope line with the dual-linear flow, radial flow and parabolic flow lines: t_{SS2PBi} and t_{SS2DLi}. Read

the intersection point of the dual linear line with the -1-slope line, t_{SS2DLi} and find X_E with Eq. 40. Also, read the intersection point of the radial with the straight line of slope=-1, t_{SS2Ri} and find X_E with Eq. 41. Estimate drainage area from: $A = X_E * Y_E$.

Step 16: Well is off-centered and both extreme boundaries are constant-pressure lines. Read the intersection point of the striagth line of slope =-1 (which is observedonly after reaching the open boundary) dual-linear and the parabolic flow lines: t_{SS1PBi} and t_{SS1DLi} and estimate the reservoir length, X_E, using Eq. 39 and 40. When the dual linear flow is not present (for small X_E/Y_E ratios) X_E can be estimated, using Eq. 38, from the intersection of the straight line of slope=-1 and the radial flow line t_{SS1Ri}. Also, read the intersection point of the parabolic line with the straight line of slope=-1 , t_{SS1PBi} and find X_E with Eq. 39. Estimate drainage area by multiplying $X_E * Y_E$.

EXAMPLES

Example 1: A synthetic test was run with the information of Table 1. The pressure and pressure derivative plot is given in Fig. 8. From there, the following characteristic points were read:

t_r = 0.18 h	ΔP_r = 5.275 psi	$(t^*\Delta P')_r$ = 0.36 psi
t_{DL} = 0.9 h	ΔP_{DL} = 5.92 psi	$(t^*\Delta P')_{DL}$ = 0.532 psi
t_{RDLi} = 0.4815 h	t_{DLPi} = 5.348 h	t_{RPi} = 1.605 h

The calculation results are presented below following the step-by-step procedure:

Step	Parameter	Equation	Value	Average
3	$\bar{k}$, md	19	1414	
3	s_m	57	0.56	
4	k_y, md	22	501.4	
5	k_z, md	4	3980.5	
6	k_x, md	24	3781.5	3881
7	s_{DL}	59	30.77	
8	b_x	$0.5X_E$	4667.9	From step 9
9	A, ft^2	30	9398903.96	
9	A, ft^2	31	9271889.64	9335396.8
9	X_E, ft	A/Y_E	9335.4	
10-13	Do not apply			
14	s_t	61	31.33	
15-16	Do not apply			

Table 1: Reservoir, well and fluid parameters for examples

	Example 1	Example 2	Example 3
Parameter	Value		
q (BPD)	300	300	500
h (ft)	100	100	30
c_t (psi^{-1})	2×10^{-6}	2×10^{-6}	1×10^{-5}
r_w (ft)	0.5	0.5	0.33
ϕ (%)	20	20	20
B, (bbl/STB)	1.2	1.2	1.1
μ (cp)	2	2	1.4
Y_E (ft)	1000	1000	300
X_E (ft)	10000	10000	
b_x (ft)	5000	2000	530
b_y (ft)			100
k_x (md)	4000	500	
k_y (md)	500	4000	
A			10
s_m	0	0	

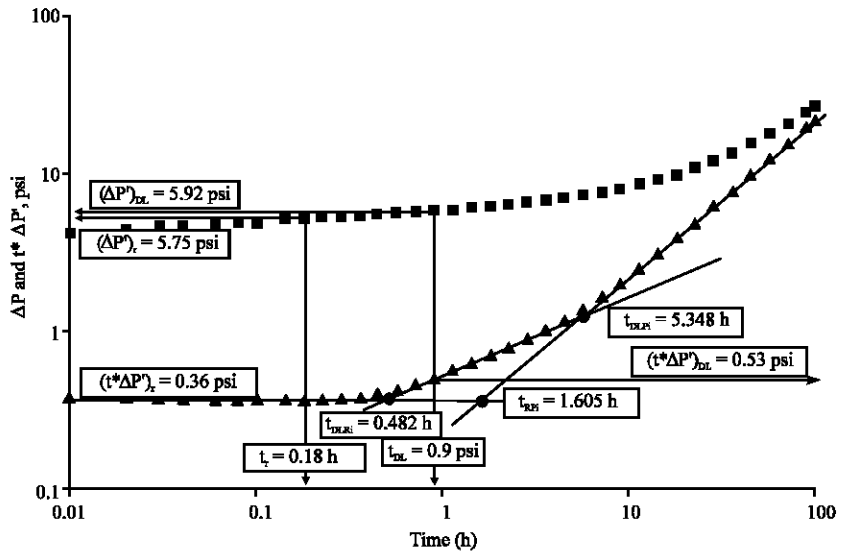

Fig. 8: Pressure and pressure derivative for example 1

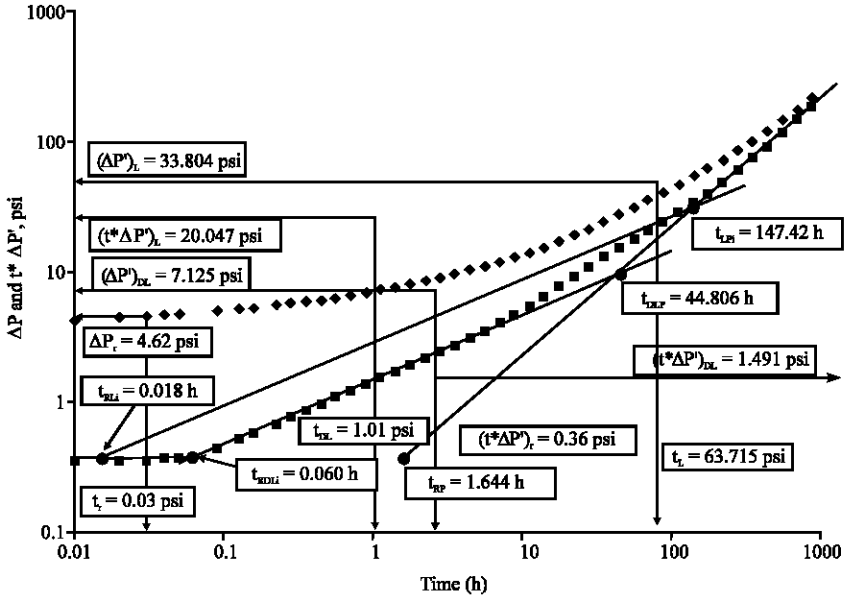

Fig. 9: Pressure and pressure derivative for example 2

Example 2: Another simulated example was run with the information of Table 1. The pressure and pressure derivative plot is shown in Fig. 9. The characteristic points given below were read from Fig. 9.

t_r = 0.03 h	ΔP_r = 4.62 psi	$(t*\Delta P')_r$ = 0.3601 psi
t_{DL} = 1.01 h	ΔP_{DL} = 7.125 psi	$(t*\Delta P')_{DL}$ = 1.49 psi
t_L = 63.715 h	ΔP_L = 33.804 psi	$(t*\Delta P')_L$ = 20.047
psit$_{RDLi}$ = 0.0603 h	t_{RLi} = 0.0183 h	t_{DLPi} = 44.806 h
t_{LPi} = 147.421 h	t_{RPi} = 1.644 h	t_F = 31.933 h
	$(t*\Delta P')_F$ = 11.94 psi	

The calculation results are summarized below:

Step	Parameter	Equation	Value	Average
3	$\bar{k}$, md	19	1411.66	
3	s_m	57	0	
4	k_y, md	22	4003.6	
4	k_y, md	23	3937.05	3988.3
5	k_x, md	4	499.7	
6	k_x, md	24	486.2	
6	k_x, md	25	533.09	506.33
7	s_{DL}	59	3.59	
7	s_L	58	-1.81	
8	b_x, ft	44	1926.1	
9	A, ft^2	30	9612568.7	
9	A, ft^2	31	9693985.8	
9	A, ft^2	32	9920565.6	9742373.4
9	X_E, ft	A/Y_E	9742.4	
10-13	Do not apply			
14	s_t	61	1.78	
15-16	Do not apply			

Example 3: The pressure and pressure derivative data in Fig. 10 were presented by Sui *et al.* (2007) for an off-entered well. Other relevant data are given in Table 1. The characteristic points given below were read from Fig. 10.

t_r = 0.042 h	t_{re} = 0.072 h	ΔP_r = 29.4 psi
$(t*\Delta P')_r$ = 2.6 psi	t_{DL} = 0.35 h	ΔP_{DL} = 35 psi
$(t*\Delta P')_{DL}$ = 4.05 psi	t_{PB} = 10.77 h	ΔP_{PB} = 50.03 psi
$(t*\Delta P')_{PB}$ = 2.49 psi	t_{RPBi} = 9 h	t_{DLPBi} = 1.1 h

The calculation results are summarized below:

Step	Parameter	Equation	Value	Average
3	$\bar{k}$, md	19	697	
3	s_m	57	0.35	
4	k_y, md	69	368.7/cos$^2\beta$	
5	Skipped			
6	k_x, md	24	921.3	
6	k_{max}, md		2150	Application of Eq. 68 is given below
6	k_{min}, md		228	
6	θ, degrees		22	
6	β, degrees		68	
4	k_y, md		2627.4	
7	s_{DL}	59	121.2	
7	s_{PB}	60	13.98	
8	Does not apply			
9	Does not apply			
10	Does not apply			
11	b_x, ft	51	308.5	
11	b_x, ft	52	354.7	
12	b_x, ft	28	302.96	
13	b_x, ft	33	290.9	
13	b_x, ft	34	257.5	302.4
13	s_{PB}	60	13.98	
14	s_t	62	14.33	
14-16	Do not apply			

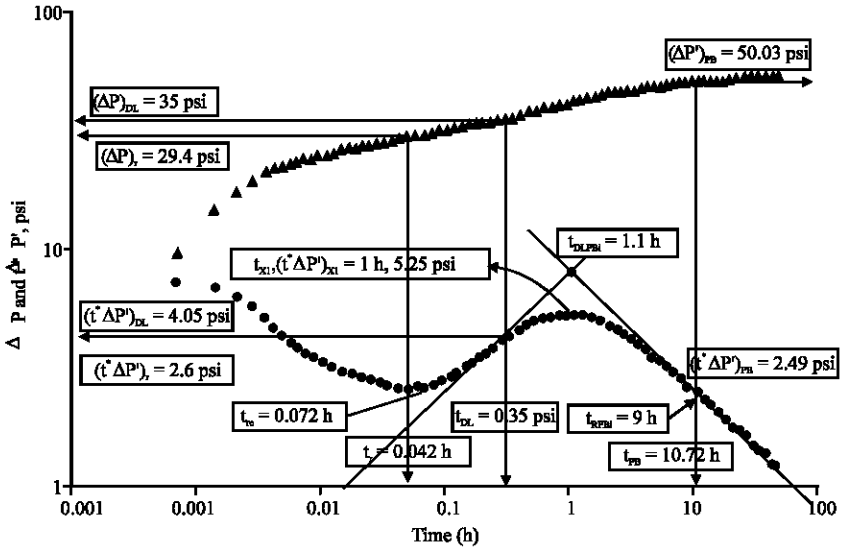

Fig. 10: Pressure and pressure derivative for example 3

$$\begin{cases} \dfrac{\cos^2\beta}{368.7} = \dfrac{\cos^2(\theta-\beta)}{k_{max}} + \dfrac{\text{sen}^2(\theta-\beta)}{k_{min}} \\ \dfrac{1}{921.3} = \dfrac{\sin^2(\theta \pm \pi/2)}{k_{max}} + \dfrac{\cos^2(\theta \pm \pi/2)}{k_{min}} \\ 697 = \sqrt{k_{Hmax} k_{Hmin}} \\ \dfrac{k_{min}}{k_{max}} = \dfrac{\tan(\theta-\beta)}{\tan\theta} \end{cases}$$

Up to step 6, Sui *et al.* (2007) reported values with good agreement to the values estimated here. Using the TDS technique, the estimated average well position along the x-direction b_x is 302.5 ft.

CONCLUSION

- Long and narrow reservoirs formed by either faulting or fluvial deposition are common in the three Basins of the Magdalena River Valley in Colombia in Columbia and worldwide.
- Several flow regimes may develop in these systems: Linear, dual-linear, parabolic, constant-pressure line, radial and pseudosteady state.
- Analytical equations corresponding to each flow regime have been derived. These flow regimes may be identified by their characteristic straight lines.
- The intersection points of these flow regime straight lines yield unique equations which can be used to calculate various parameters or for verification purposes.
- A finding of major importance is that areal anisotropy can be characterized from a pressure buildup or pressure drawdown test in a single vertical well if the reservoir width is known from other sources.
- It is important to run a long test in order to observe the radial, linear and dual-linear flow regimes to calculate the x and y directions permeabilities.
- The length and width of the reservoir can be determined from the pressure test if the pseudosteady state is observed. Otherwise, it must be estimated from seismic data.

Nomenclature:

A	:	Area, ft^2
B	:	Oil formation factor, bbl/STB
b_x	:	Actual distance from well to the closest lateral boundary along the x-direction, ft
b_x'	:	Distance from well to the closest lateral boundary (along the x-direction) affected by anisotropy, ft
b_x	:	Actual distance from well to the closest lateral boundary along the y-direction, ft
b_x'	:	Distance from well to the closest lateral boundary (along the y-direction) affected by anisotropy, ft
c_t	:	Compressibility, 1/psi
h	:	Formation thickness, ft
$\bar{k}$	:	Mean geometric permeability or areal permeability, md
$\bar{k}_1$	:	k_y, md
$\bar{k}_2$	:	k_x, md
k_{max}	:	Horizontal maximum principal permeability, md
k_{min}	:	Horizontal minimum principal permeability, md
k_x	:	Permeability in x-direction, md
k_y	:	Permeability in y-direction, md
P	:	Pressure, psi

P_D' : Dimensionless pressure derivative
P_D : Dimensionless pressure
P_i : Initial reservoir pressure, psia
P_e : External reservoir pressure, psia
P_{wf} : Well flowing pressure, psi
q : Flow rate, bbl/D. For gas reservoirs the units are Mscf/D
r_D : Dimensionless radius
r_e : Drainage radius, ft
r_w : Well radius, ft
s : Skin factor
s_t : Total skin factor
T : Reservoir temperature, °R
t : Time, hr
t*Δm
(P)' : Pseudopressure derivative function, psi^2/cp
t_D : Dimensionless time
X_E : Reservoir length, ft
Y_E : Actual reservoir width, ft

REFERENCES

Ayestaran, L.C., R.D. Nurmi, G.A.K. Shehab, and W.S. El Sisi, 1989. Well Test Design and Final Interpretation Improved by Integrated Well Testing and Geological Efforts. Paper SPE 17945, Proceedings, SPE Middle East Oil Technical Conference and Exhibition, Manama, Bahrain.

Bendekim, G., D. Tiab and F.H. Escobar, 2002. Pressure Behavior of a Well in an Anisotropic Reservoir. Paper SPE 76772, SPE Western Regional/AAPG Pacific Section Joint Meeting held in Anchorage, Alaska, U.S.A.

Escobar, F.H., O.F. Munoz, J.A. Sepulveda and M. Montealegre, 2005. New Finding on Pressure Response. In Long, Narrow Reservoirs. Ct and F-Ciencia, Tecnología y Futuro, Vol. 2.

Escobar, F.H., Y.A. Hernandez and C.M. Hernandez, 2007. Pressure Transient Analysis for Long Homogeneous Reservoirs using TDS Technique. Journal of petroleum Science and Engineering. Available in Science Direct.com Since.

Her-Yuan, C. and W.T. Lawrance, 2000. A Quick Method to Diagnose Flow Anisotropy using Pressure Interference Data. Paper SPE 60290 presented at the 2000 Regional Symposium of Low Permeability reservoirs held in Denver, CO.

Hsing, Hsu H., 1979. Analysis of Flow Mixed Boundary Systems by Type Curve Matching. MS Thesis, The University of Oklahoma, pp: 185.

Nutakki, R. and L. Mattar, 1982. Pressure Transient Analysis of Wells in Very Long Narrow reservoirs. Paper SPE 11221, presented at the 57th Annual Fall Technical Conference and Exhibition of the Society of Petroleum Engineers held in Dallas, TX.

Sui, W., J. Mou, L. BI, J. Den and C. Ehlig-Economides 2007. New Flow Regimes for Well Near-Constant-Pressure Boundary. Paper SPE 106922, proceedings, SPE Latin American and Caribbean Petroleum Engineering Conference, Buenos Aires, Argentina.

Tiab, D. and H. Chrichlow, 1979. Analysis of Multiple-Sealing Fault Systems and Bounded Reservoirs by Type Curve Matching. Soc. Petroleum Eng. J., pp: 378-392.

Tiab, D., 1975. A New Approach (pressure derivative) to Detect and Locate Multiple Reservoir Boundaries By Transient Well Pressure Data. M.S. Thesis, New Mexico Tech., pp: 137.

Tiab, D., 1976. Analysis of Multiple-Sealing Faults Systems and Bounded Reservoirs by Type-Curve Matching (using pressure and pressure derivative). Ph.D. Dissertation, University of Oklahoma, pp: 235.

Tiab, D., 1993. Analysis of Pressure and Pressure Derivative without Type-Curve Matching: 1- Skin and Wellbore Storage. J. Petroleum Sci. Eng., 12: 171-181.

Tiab, D., 1995. Analysis of Pressure and Pressure Derivatives without Type-Curve Matching-III. Vertically Fractured Wells in Closed Systems. Paper SPE 26138, SPE Western Regional Meeting, Anchorage, Alaska.

Tiab, D., A. Azzougen, F.H. Escobar and S. Berumen, 1999. Analysis of Pressure Derivative Data of a Finite-Conductivity Fractures by the 'Direct Synthesis Technique. Paper SPE 52201 presented at the 1999 SPE Mid-Continent Operations Symposium held in Oklahoma City, OK, March 28-31, 1999 and presented at the 1999 SPE Latin American and Caribbean Petroleum Engineering Conference held held in Caracas, Venezuela.

Wong, D.W., C.D. Mothersele, A.G. Harrington and H. Cinco-Ley, 1986. Pressure Transient Analysis in Finite Linear Reservoirs Using Derivative and Conventional Techniques: Field Examples. Paper SPE 15421, 61st Annual technical Conference and Exhibition of the Society of Petroleum Engineers held in New Orleans, LA.